# Classical Analysis of Phenomenological Potentials for Metallic Clusters

W. D. Heiss[1] and R. G. Nazmitdinov[2,*]

[1]*Centre for Nonlinear Studies and Department of Physics, University of the Witwatersrand, PO Wits 2050, Johannesburg, South Africa*

[2]*Departamento de Fisica Teorica C-XI, Universidad Autonoma de Madrid, E-28049, Madrid, Spain*

(Received 11 April 1994)

The classical trajectories of single particle motion in a Woods-Saxon and a modified Nilsson potential are studied for axial quadrupole deformation. Both cases give rise to chaotic behavior when the deformation in the Woods-Saxon and the $\vec{l}^2$ term in the modified Nilsson potential are turned on. Important similarities, in particular with regard to the shortest periodic orbits, have been found.

PACS numbers: 36.40.+d, 05.45.+b

Recent experimental results on metallic clusters reporting abundance variations in mass spectra, ionization potentials, static polarizabilities and collective giant dipole resonances, barrier shapes, and fragmentation provide us with striking manifestations of shell structure effects related to a quantized motion of the valence electrons [1]. The correspondence of the electronic shell structure in spherical clusters to the closing of major quantal shells [2–4] caused considerable interest in using nuclear shell model type calculations for the description of metallic clusters [5–9]. It turns out that phenomenological potentials used traditionally in nuclear physics serve a purpose similar to those obtained within the Kohn-Sham density-functional method [10] if the relevant parameters are adjusted appropriately. Typical potentials are the Woods-Saxon (and its various modifications) and the modified Nilsson potential without spin-orbit term. The considerable lowering of the computational time due to their simple analytical form renders an analysis of the stability of large metallic clusters feasible. Naturally, the shell numbers have to be larger than the ones used in nuclear physics in accordance with the larger number of valence electrons considered for metallic clusters. For mesoscopic objects like clusters, deformations, i.e., deviations from spherical symmetry of the potential, are as important as in the nuclear physics context. Metallic clusters can be seen as a "gift of nature" towards a deeper understanding of the formation of shell and supershell structure which is a general feature for any self-consistent theory of independent particles moving in an average potential.

The existence of shell structures is one of the crucial questions addressed by previous [5,6,7,9,11] and more recent authors [12–14]. Obviously, shell structure in the quantum mechanical spectrum is associated with periodic orbits in the corresponding classical problem [15,16]. Furthermore, if the corresponding classical problem is nonintegrable and displays chaotic behavior, the shell structure of the corresponding quantum spectrum is affected depending on the degree of chaos [17,18]. Since the deformed Woods-Saxon potential as well as the modified Nilsson potential are nonintegrable systems, a classical analysis of the single particle motion seems to be indicated to shed light on the corresponding quantum mechanical problem. Results of such analysis are presented in this paper. This is relevant for two reasons. Since the Woods-Saxon potential and the Nilsson model are both used with success in quantum mechanical models for clusters, it is of interest to look at their similarities in the classical context; in fact, their similarities are not obvious at first glance. Furthermore, since the two models show chaotic behavior as is demonstrated below, it is essential to understand whether at least the shortest periodic orbits have similar features; otherwise, the corresponding quantum problem is unlikely to agree with regard to shell structures. In fact, it is the shortest orbits with smallest period that make the most important contribution to shell structure in the quantum spectrum [16].

We investigate the classical single particle motion for the Hamiltonian function (we put the mass equal to unity)

$$H = \tfrac{1}{2}(p_r^2 + p_\theta^2/r^2) + V_{\mathrm{WS}}(r,\theta), \tag{1}$$

where we used the deformed Woods-Saxon potential $V_{\mathrm{WS}}(r,\theta) = V_0/(1 + \exp\{[r - R(\theta)]/d(\theta)\})$ with $R = R_0[1 + \alpha P_2(\cos\theta)]$ and $d = d_0[1 + (\nabla R)^2/2R^2]$ [15], where $P_2$ is the second order Legendre polynomial and $\alpha$ a deformation parameter. As a second case we consider the classical analog of the quantum mechanical Nilsson Hamiltonian (neglecting the spin-orbit term)

$$H = \tfrac{1}{2}(p_\varrho^2 + p_z^2) + \tfrac{1}{2}(\omega_\perp^2 \varrho^2 + \omega_z^2 z^2) + \lambda(\varrho p_z - z p_\varrho)^2. \tag{2}$$

In both cases there is cylindrical symmetry. We restrict ourselves to zero value for the $z$ component of the angular momentum, that is, $p_\phi = \phi r^2 \sin^2\theta = 0$; we have left out the $\phi$ dependence altogether. We have chosen cylindrical coordinates $\varrho$ and $z$ in the second case while the choice $r = \sqrt{\varrho^2 + z^2}$ and $\theta$ with $\tan\theta = \varrho/z$ is more appropriate in the first case.

We first consider qualitatively the case of spherical symmetry which means $\alpha = 0$ in the first and $\omega_\perp = \omega_z$

0031-9007/94/73(9)/1235(4)$06.00

in the second case. Both cases reduce to 1 degree of freedom since now $p_\theta = \dot{\theta} r^2 = z p_\varrho - \varrho p_z$ is conserved. Closed orbits occur if the radial and angular frequencies are commensurate. Rewriting Eq. (2), for $\omega_\perp = \omega_z$, as $H = \frac{1}{2}(p_r^2 + p_\theta^2/r^2) + \frac{1}{2}\omega_z^2 r^2 + \lambda p_\theta^2$ we obtain closed orbits if $\lambda p_\theta/\omega_z + 1/2 = n/m$ with integers $n$, $m$. For instance, when $n/m = 1/3, 1/4, \ldots$, the trajectory forms essentially a triangle, a square, etc. in the $\varrho$-$z$ plane; for $n/m = 2/5$ we get the five star, and so forth. The precise shapes of these geometrical figures depend on the magnitude of $\lambda$ in that small values of $\lambda$ produce polygons with rounded corners while larger values yield loops at the corners as is illustrated in Fig. 1. The appropriate scaling of $\lambda$ is given by the kinematical constraint between the energy and the angular momentum which reads $E - \lambda p_\theta^2 \geq \omega |p_\theta|$. Here we emphasize that for negative values of $\lambda$, as used in actual applications, the value of the angular momentum $p_\theta$ is not limited in its absolute value for a given energy. In particular, the relation implies that (for $\lambda < 0$) if $4|\lambda| > \omega^2/E$ there is no restriction at all on $p_\theta$. For the Hamiltonian function of Eq. (1) an appropriate choice of $p_\theta$ can likewise lead to polygon orbits such as a triangle, square, pentagon, but also a five star, and so forth. The corners of the polygons are increasingly sharp the smaller the value of the diffuseness $d_0$ (or the larger the value of $R_0$). The angular momentum $p_\theta$, and therefore the number of corners of the polygons, is now limited by the kinematical constraint $p_\theta^2 \leq \max_r(2r^2[E - V_{\mathrm{WS}}(r,0)])$. The plain circle (polygon of infinitely many corners) is possible only for zero diffuseness where the maximum is reached at $r = R_0$.

Thus a common feature of the two Hamiltonian functions is, for the trivial spherical case, the existence of closed orbits of simple geometric shapes. Such closed orbits have been observed by other authors for the Woods-Saxon potential [6,12,13] but not, to the best of our knowledge, for the Nilsson Hamiltonian under consideration. As indicated above, there is, however, a crucial difference between the two: the phase space is noncompact for the second case if $\lambda < 0$. When deformation is invoked both problems become nonintegrable as $p_\theta$ is no longer conserved. The symmetrical periodic orbits discussed above are destroyed. The onset of chaotic motion can be discerned; for small deformation this happens only in parts of phase space.

For the Woods-Saxon potential we have chosen only a quadrupole deformation of the boundary $R$. The deformation of the diffuseness is a consequence of volume conservation [15]. Note that a pure quadrupole deformation of a cavity ($d_0 = 0$) yields an integrable case [19] for the bound state problem. In our case, when $\alpha$ is turned on, the effective deformation of $V_{\mathrm{WS}}(r,\theta)$ implies higher multipoles of order $2^{2l}$, $l = 1, 2, 3, \ldots$, since $V_{\mathrm{WS}}(r,\theta)$ can be expanded in terms of even order Legendre polynomials. The presence of higher multipoles is expected to lead to chaotic behavior [20]. Results of our analysis confirm this expectation. We have solved numerically the canonical equations of motion and obtained surfaces of section in the plane $\varrho = 0$; i.e., the phase space diagrams displayed in Fig. 2 are in the $z$-$p_z$ plane. Our results are general; for demonstration we have chosen the parameters $V_0 = -6$ eV, $d_0 = 0.74$ Å, $R_0 = 15$ Å, and $-3$ eV for the energy; this corresponds to the Fermi level of a cluster with 300 particles [6]. Figure 2(a) represents sections of three orbits; the initial values of the one in the center have been chosen to display the separatrix that separates

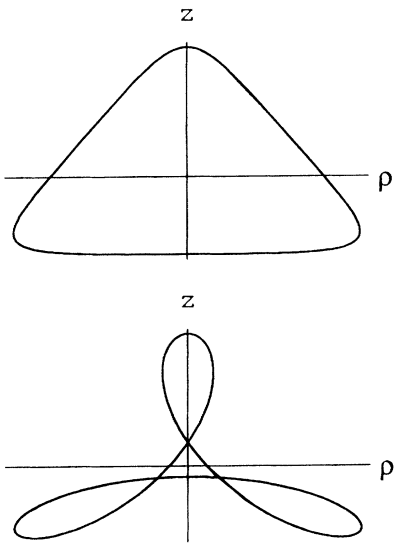


FIG. 1. Typical simple periodic orbits for the spherical Nilsson model. The orbit with the loops at the corners is for $|\lambda| \gtrsim \omega^2/4E$ while the other one is for $|\lambda| = \omega^2/25E$.

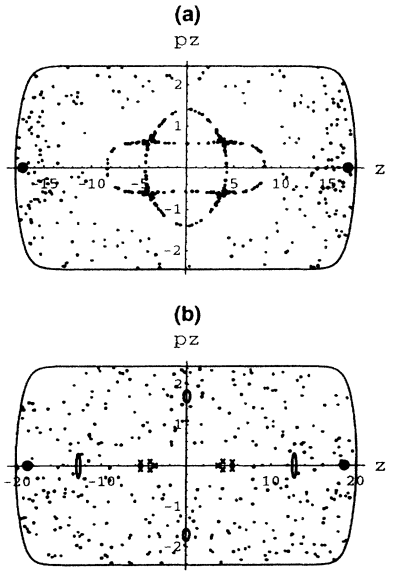


FIG. 2. Surfaces of section for the deformed Woods-Saxon potential for $\alpha = 0.1$ (top) and $\alpha = 0.16$ (bottom).

a periodic orbit whose trajectory is displayed in Fig. 3(b), and a vibrational mode in the center of the $z$-$p_z$ plane of Fig. 2(a). For this particular value of $\alpha$ the motion is still regular in most parts of the accessible phase space. Another periodic orbit with small stability islands exists at $z = \pm 17.2$ and $p_z = 0$; it is indicated by a pronounced solid dot and its trajectory is displayed in Fig. 3(a). Only this and the orbit associated with the outer part of the separatrix can still be traced when $\alpha$ is increased from 0.1 to 0.16, but only the islands surrounding the latter are still significant while the ones at the fringes of phase space ($z = \pm 18.7$) have virtually shrunk to zero; this is illustrated in Fig. 2(b). The onset of chaos now occupies larger parts of the phase space. The fast decay of the stability islands for only a small range of $\alpha$ values is remarkable. The center range in Fig. 2(b) is still associated with quasiperiodic motion. There are many long time periodic orbits which emerge from the center. The shortest ones are indicated by crosses and their trajectories are illustrated in Figs. 3(c) and 3(d). The most stable and shortest periodic orbit in Fig. 2(b) is associated with the islands drawn; the trajectory remains that of Fig. 3(b). Hard chaos takes over all of phase space when $\alpha$ is further increased. The range of $\alpha$ values considered here is in line with values used by other authors [7]. We mention that omission of the $\theta$ dependence of the diffuseness, i.e., putting $d \equiv d_0$, does not change the qualitative picture of the surfaces of section; it does, however, drastically change an individual chaotic orbit. All orbits displayed in Fig. 3 emerge from the center of the surfaces of section with increasing $\alpha$. While they move outwards in the section with increasing $\alpha$ their corresponding stability region shrinks until it disappears.

For the Nilsson Hamilton function of Eq. (2) deformation is invoked by choosing $\omega_\perp > \omega_z$. The inequality is associated with prolate deformation. In our context this is the only case of importance since oblate deformation is related to prolate by interchanging $\varrho$ and $z$. When $\lambda = 0$ and $\omega_\perp > \omega_z$ the orbits are Lissajou figures; closed orbits are obtained for commensurate $\omega_\perp$ and $\omega_z$. Our interest is directed towards short periodic orbits for $\lambda \neq 0$ where we actually focus on $\lambda < 0$ because of its physical relevance. We have investigated the range of the parameter $b$, defined by $\omega_\perp = b\omega_z$, in the interval $1.5 \leq b \leq 2$. Figure 4(a) displays the phase space structure at $\varrho = 0$ where the surfaces of section are taken. Note that for $\lambda < 0$, the whole region to the left and right, i.e., outside the lines $z = \pm\sqrt{1/2|\lambda|}$, is accessible as long as the two lines do not intersect with the ellipse which forms the other part of accessible phase space; if $|\lambda|$ is sufficiently large to allow intersection of the lines with the ellipse, the phase space becomes connected; then the part of the ellipse which is to the left and right of the lines is inaccessible. In Fig. 4(b) surfaces of sections for $\lambda = -0.01$ are given for four different orbits. With the choice of energy $E = 50$ and the frequency $\omega_z = \pi/2$ the two lines are outside the ellipse. Recall that the same pattern is obtained if $E$ and $\lambda$ are rescaled such that $E\lambda = \text{const}$. With regard to periodic orbits there is a remarkable similarity between Figs. 2(b) and 4(b). In fact, the short periodic orbits are of the same geometrical shape and occur in similar regions of the surfaces of section. Compare in particular the rather stable orbit of Fig. 4(b) with the corresponding orbit in Fig. 2(b); both have the same trajectory [Fig. 3(b)] and their stability islands are situated in a chaotic region; further the orbits of Figs. 3(c) and 3(d) in the center of the phase diagram which forms the stable region of Figs. 2(b) and 4(b); and the orbit of Fig. 3(a) which is situated on the fringes of phase space within a tiny region of stability. The diagram of Fig. 4(b)

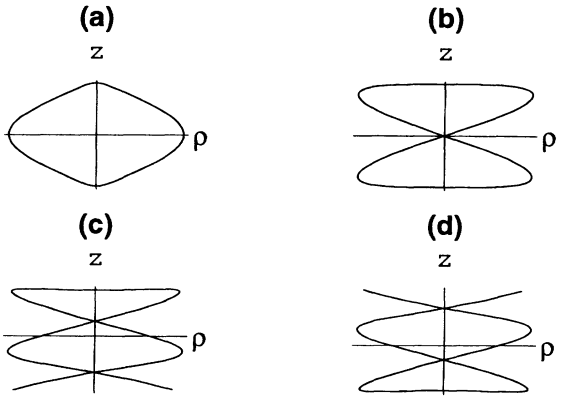


FIG. 3. Typical short periodic orbits for the deformed Woods-Saxon potential in the $\varrho$-$z$ plane. The same shapes occur in the modified Nilsson model. (c), (d) Self-tracing orbits.

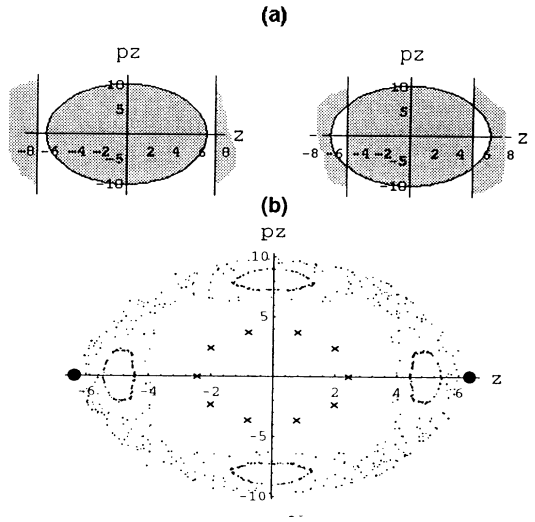


FIG. 4. Surfaces of section for the modified Nilsson model. In (a) two situations of accessible phase space (shaded) are displayed; left: $|\lambda| < \omega_z^2/4E$; right: $|\lambda| > \omega_z^2/4E$. Four orbits for a value of $\lambda$ which corresponds to the left of (a) are displayed in (b).

refers to $b = 2$, but the pattern as described prevails for $1.5 < b \leq 2$. For larger values of $|\lambda|$ hard chaos takes over quickly within the ellipse, in particular, when the two lines enter the ellipse. However, regular motion prevails outside the ellipse which is the whole area to the left of the left line and to the right of the right line. These orbits may attain large values of $\varrho$ and $z$; also the variation of the angular momentum $p_\theta$ is unlimited in principle. In this context we stress that the variation of $p_\theta$ ranges typically between $-50$ and $+50$ for generic orbits inside the ellipse for our choice of parameters. This is significant when considering a corresponding quantum mechanical calculation.

To summarize, the deformed Woods-Saxon potential and the modified Nilsson model are both used in quantum mechanical models, more recently in application to metallic clusters. Their classical analogs do not appear to have much in common at first sight, yet we have established important similarities between the two. While this provides confidence in the quantum mechanical approach where the two models are used for similar purposes, our results also call for a certain caution. Both models are potentially chaotic with the degree of chaos depending on the deformation parameter in the Woods-Saxon potential or on the parameter $\lambda$ in front of the $\vec{l}$ term present in the Nilsson model. Within the context of nuclear physics this behavior is probably of little significance, since only the lower end of the spectrum is of interest. For metallic clusters, however, with the much larger particle numbers, a higher range of the spectrum becomes relevant; in this region chaotic behavior may well interfere with the search for shell structure. Our results suggest that electronic shell structure is not expected to play a major role for the stability and formation of metallic clusters if a substantial deformation prevails; however, in previous results, where odd order multipoles were considered [18], the very existence of shell structure was pointed out for prolate deformation. Further investigations have to provide clarity on this aspect. Finally we point out that, in view of the large fluctuations in time of the classical angular momentum $p_\theta$, a too severe truncation in the corresponding (stationary) quantum mechanical calculation could easily invalidate results—in particular, it could conceal the onset of chaos in the quantum spectrum.

R. G. N. gratefully acknowledges financial support from DGICYT of Spain.

*On leave of absence from Joint Institute for Nuclear Research, Bogoliubov Laboratory of Theoretical Physics, 141980 Dubna, Russia.

[1] W. A. Heer, Rev. Mod. Phys. **65**, 611 (1993); M. Brack, *ibid.* **65**, 677 (1993).
[2] S. Bjornholm *et al.*, Phys. Rev. Lett. **65**, 1627 (1990).
[3] C. Brechignas *et al.*, Phys. Rev. B **47**, 2271 (1993).
[4] T. P. Martin *et al.*, Chem. Phys. Lett. **186**, 53 (1991).
[5] K. Clemenger, Phys. Rev. B **32**, 1359 (1985).
[6] H. Nishioka, K. Hansen, and B. R. Mottelson, Phys. Rev. B **42**, 9377 (1990).
[7] S. Frauendorf and V. V. Pashkevich, Z. Phys. D **26**, S98 (1993).
[8] C. Yannouleas and U. Landman, Phys. Rev. B **48**, 8376 (1993).
[9] A. Bulgac and C. Lewenkopf, Phys. Rev. Lett. **71**, 4130 (1993).
[10] W. Kohn and L. J. Sham, Phys. Rev. **140**, 1133A (1965).
[11] K. Clemenger, Phys. Rev. B **44**, 12991 (1991).
[12] J. Mansikka-ako, M. Manninen, and H. Nishioka, Phys. Rev. B **48**, 1837 (1993).
[13] J. Lerme *et al.*, Phys. Rev. B **48**, 9028 (1993).
[14] N. Pavloff and S. C. Creagh, Phys. Rev. B **48**, 18164 (1993).
[15] A. Bohr and B. R. Mottelson, *Nuclear Structure* (Benjamin, New York, 1975), Vol. 2.
[16] V. M. Strutinsky and A. G. Magner, Sov. J. Part. Nucl. **7**, 138 (1976).
[17] M. C. Gutzwiller, *Chaos in Classical and Quantum Mechanics* (Springer Verlag, New York, 1990).
[18] W. D. Heiss, R. G. Nazmitdinov, and S. Radu, Phys. Rev. Lett. **72**, 2351 (1994).
[19] R. Arvieu, F. Brut, J. Carbonell, and J. Touchard, Phys. Rev. A **35**, 2389 (1987).
[20] J. Blocki, J.-J. Shi, and W. J. Swiatecki, Nucl. Phys. **A554**, 387 (1993).

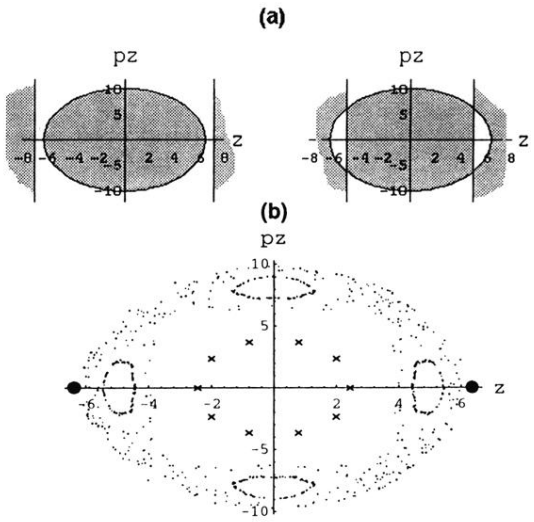


FIG. 4. Surfaces of section for the modified Nilsson model. In (a) two situations of accessible phase space (shaded) are displayed; left: $|\lambda| < \omega_z^2/4E$; right: $|\lambda| > \omega_z^2/4E$. Four orbits for a value of $\lambda$ which corresponds to the left of (a) are displayed in (b).